Chapter 7

Skin Wound Healing Revealed by Multimodal Optical Microscopies

Gitanjal Deka, Shi-Wei Chu and Fu-Jen Kao

Additional information is available at the end of the chapter

http://dx.doi.org/10.5772/64088

Abstract

Skin is the largest organ of our body serving as the first line defense against pathogens and toxicity. The skin can heal itself if any damage in it occur. Wounds, if not taken care properly, can become chronic and can even cause death. In the field of cosmetics and plastic reconstructive surgery, wounds, are major cause of trauma and costs, which demand proper diagnosis that can help in appropriate treatment. In conventional medicine, wound diagnosis mostly relied on the expertise and experience of physicians on the basis of non-quantitative observation of clinical signs, or invasive histochemical assessment of biopsies.

Methodologies based on light-matter interaction can provide quantitative, noninvasive and real time assessment of a tissue section based on imaging. Depending on the nature of interaction, various contrasts can be achieved by either absorption, scattering, or fluorescence, enabling observation of structural or molecular components of tissue sections. Development of multiphoton nonlinear optical detection techniques provide better resolution and tissue penetration depth with optical sectioning ability by using molecular and structural contrasts simultaneously. This chapter discuses and evaluates various optical approaches with special emphasis on multimodal multiphoton imaging of skin tissue components in correlation to physiological processes that affects the wound healing.

Keywords: skin, wound healing, optical microscopy, NADH, collagen, fluorescence, second harmonic generations

1. Introduction

Skin wounds and their treatment lead to major medical expenses in cosmetic surgery. Chronic wounds, including diabetic ulcers and pressure ulcers, present a significant health and economic concern for individual patients as well as the healthcare system. The diabetic ulcer is a major complication of diabetes mellitus, a disease which afflicts more than 350 million people worldwide. Among them foot ulceration is the leading cause for hospitalization [1]. Acute cutaneous burn wounds are also a serious health-related issue in the global community. Nearly 11 million flame burns occur annually and burn deaths rank in the top 15 causes of death for individuals 5–29 years of age. Around 60% of these burn patients heal with debilitating hypertrophic or keloid scarring [2]. Additionally, the cutaneous burn wound can left deep and large scar in comparison to normal wound after healing. All these scars are formed due to over deposition of collagen fibers to fill up the wound gaps, which are structurally and molecularly different to each other and need different approaches for their diagnosis and management. Improper management of wound may cause serious tissue disfigurement that may cause serious physical and psychological problems in patients.

Wound healing is a widely studied biomedical problem regarding tissue systems. To address the situation of wounds and their assessment of healing potential requires insight of what occurs to the components of skin at cellular and molecular level. Specifically, epithelial cell migration and collagen regeneration by fibroblast cells in the skin were found to have great effects on accelerated wound healing [3]. The entire wound healing process is a complex series of events that starts at the moment of injury and can continue for months even years in a few sequential yet overlapping phases. The characterization of wounds, their healing, and also the timeline of these sequential phases have major clinical significance in assessing severity, healing potential, and determining the correct treatment for all wound types. Traditionally, wound assessment has relied on visual evaluation by trained clinicians, with techniques based on laboratory biopsies providing objective assessment modalities [4, 5]. Currently, histological analysis of the tissue remains the gold standard for precise quantitative and qualitative assessment of wound depth and status. However, the biopsy process is invasive, can be painful, and in some cases can cause additional trauma and worsen scarring [4, 5]. Additionally, the processing required for histochemical observation usually distorts the structural integrity of the tissue.

In contrast to the abovementioned traditional wound assessment procedures, noninvasive imaging by optical means does not require destructive tissue sectioning; it preserves all layers of the skin. By collecting the information through light and tissue interaction, optical imaging assesses wound severity, healing potential, and progress in a rapid, objective, and noninvasive manner. Optical microscopic techniques use various biomolecules as marker to observe skin and its physiology. Various imaging modalities detect scattering and absorption of light by these markers, aiding the qualitative and quantitative evaluation of cell regeneration, metabolic activity, collagen remodeling, blood flow, inflammation, vascular structure, and water content. For example, absorption by hemoglobin provides contrast of veins in technique such as laser Doppler imaging (LDI); reflection and scattering by extracellular matrix provide

structural contrast achieved by optical coherence tomography (OCT) and reflectance confocal laser scanning microscopy (RCLM) and fluorescence from molecules such as NADH, FAD [6], and tryptophan [7] provide molecular contrasts for fluorescence imaging of cells that constitute the epidermal layers of the skin. Some molecules, such as collagen and elastin found in the skin dermis, are also known to have autofluorescence [8, 9]. Along with fluorescence, collagen is better known as a strong SH generator that can provide structural contrast while imaging the dermis [9].

In clinical setting, optical imaging with these contrast mechanisms has been or has the potential to study skin wound healing noninvasively. Spectrally resolved tissue imaging with confocal or multiphoton microscopy enables 3D imaging of tissues through depth sectioning and can be used to study skin wound healing [10]. In comparison to other conventional optical microscopies, multiphoton microscopy offers a number of advantages. Nonlinear excitation limits the sample excitation to the focal volume and optical scanning with very small excitation volume results in high-contrast images. Lower scattering of IR light enables deeper penetration in tissue. Large spectral separation between the multiphoton excitation and emission provides easier discrimination of entire emission spectrum [11]. Among the modalities of multiphoton microscopy, two-photon fluorescence (2PF) and SHG present as the most effective ones in tissue imaging for diagnosis and prognosis in skin wound healing.

In this chapter we will discuss recent advancements in optical microscopic techniques for imaging skin tissue and its regeneration during wound healing. We will put forward a comparative idea of various techniques in their specific objectives of skin observations. In doing so we will briefly discuss the wound healing processes at various phases and the corresponding molecular components involved that can be used as biomarkers. Our main emphasis of the chapter is on the analysis of wound healing enabled by multiphoton microscopy (MPM), mainly 2PF and SHG imaging, and their prospects in clinical settings. However, we will also cover other popular methodologies for optical imaging of skin, highlighting their potentials in wound healing study.

2. Skin and wound healing phases

Skin is the largest organ of our body which protects us from excessive water loss and invasion of outside pathogens, senses changes in environment, etc. Before discussing the diagnostic methodologies of skin wound healing, it is very important to understand the anatomy and the molecular basis of skin and how the healing processes are related. In this section we will introduce the skin's anatomic layers and the molecules present in these layers that are potential markers for optical imaging. Various phases of wound healing and the molecular components involve in the process are also discussed in the later part of the section.

From an anatomic point of view, skin is a multilayered tissue as represented in **Figure 1(b)**. It weighs about 10% of our total body weight and thickness is approximately ranged from .5 to 2 mm [12]. The thickness of skin varies in deferent region of the body. Skin is composed of three primary layers:

(1) The epidermis, which preserves body fluid and serves as a barrier to infection, is mainly a stratified squamous epithelium composed of proliferating basal and differentiated keratinocytes. Keratinocytes are the major cells in epidermis constituting 95% of it. It is composed of five stratified layers, namely, stratum corneum, stratum granulosum, stratum spinosum, and stratum germinativum, ranging from 0.05 to 1.5 mm thick [13]. As cells possess autofluorescing chromophores, such as NADH, FAD, and tryptophan, the epidermal physiology can be observed through fluoresce microscopy.

(2) *The dermis* is the layer beneath the epidermis separated by the basement membrane and consists of connective tissues deposited in a space of 0.3–3.0 mm thickness that cushions the body from stress and strain. The connective tissues in dermis are composed mainly of extracellular matrix fibers such as elastin and collagens, ground substances, and specialized cells such as fibroblasts and adipocytes. The main components of extracellular matrix (ECM), collagen, and elastin have autofluorescence, which makes them very useful markers for wound diagnosis. However, collagen being a noncentrosymmetric molecule, SHG is the more popular way of collagen imaging. Additionally, the fibroblasts in dermis play an important role in the wound healing process, which can also be monitored with fluorescence imaging techniques [13].

Figure 1. (a) Representative image of the key players in the healing of a skin wound [3]. The wound gap is temporarily plugged with fibrin clot that protects the wound from outside environment along with providing provisions for a dense capillary plexus of new granulation tissue and inflammatory as well as fibroblast cell migration. Reconstructing epidermal cells migrates under the fibrin clot to construct the wound bed that helps in granulation tissue formation to fill the wound gap. (b) Schematic representation of skin anatomy with its different layers [25].

(3) *Hypodermis:* Hypodermis is the layer that lies below the dermis. However, it is not considered to be a part of the skin. It helps joining the skin with the underlying muscles, bones, and blood vessels, as well as nerves. It is mainly composed of loose connective tissues and elastin.

http://dx.doi.org/10.5772/64088

Fibroblasts, macrophages, and adipocytes are the main cells that comprise the hypodermis. Body fat that serves as the insulator of the body also lies in this layer [13].

In normal skin, the epidermis and dermis exist in steady-state equilibrium, forming a protective barrier against the external environment. Once the protective barrier is broken, the normal process of wound healing starts immediately. Wound healing involves sequential phases of cellular initiation and secretion of molecules triggered by specific growth factors and signaling molecules [3]. Initially, a fibrin clot is formed that plugs the defects, which provides a provisional platform for cell migration as depicted in **Figure 1(a)**. In subsequent days, the wound heals completely by forming a dynamic scar tissue rich in collagen [3]. Classical model of wound healing divides the processes into several vital sequential yet overlapping stages, such as (1) hemostasis, (2) inflammation, (3) proliferation, and (4) remodeling.

Hemostasis starts immediately after the wound formation. At this stage, blood changes from liquid state to solid state to stop excessive blood loss, which is termed as blood clotting [14, 15], followed by bacteria and cell debris at the wound site being phagocytosed and removed by macrophages and white blood cells. During this phase the wound site appears red and hotter than the adjacent area marking the onset of inflammation [16–18]. Additionally, at this stage tissue matrix metalloproteinase enzymes start to degrade surrounding ECM proteins such as collagen and necrotic cellular macromolecules to provide a platform for epithelial cells migration [3]. The proliferative phase begins only when the wound is covered by re-epithelium which will migrate to central region of the wound to cover the wound defect. Angiogenesis, collagen deposition, granulation tissue formation, epithelialization, and wound contraction are the signatures of the proliferative phase [19]. The final phase of wound healing is remodeling. It is characterized by the maturation of collagen by rearrangement, intermolecular cross-linking, and alignment along the wound tension line [16]. The remodeling phase may last for a year or even longer with respect to wound size and type [20]. As the wound maturation progresses, the tensile strength of the wound increases, ultimately becoming as strong as 80% of normal tissue [20]. The wound scar gradually flattens and becomes less prominent and more pale and supple. Since activity at the wound site is reduced, consequently blood vessels that are no longer needed are removed by apoptosis and the scar loses its red appearance [21]. The wound healing normally progresses in a predictable, timely manner if not interrupted by any means; otherwise healing may progress inappropriately to transform into a chronic wound or pathological scarring such as a keloid [22, 23]. These scars consist mainly of poorly reconstructed thick parallel bundles of collagens [24]. There are mainly three different kinds of scar tissues depending upon the deposition of ECM [24]: (a) Keloids, (b) hypertrophic scar, and (c) normal scar.

Clinically, keloids are defined as scars growing beyond the confines of original wounds, which rarely regress over time. Hypertrophic scars, on the other hand, are raised scars that remain within the boundaries of the wound and frequently regress spontaneously. Histologically, collagen bundles in the dermis of normal scar tissues appear relatively relaxed and arranged in random arrays, but keloids and hypertrophic scars have collagen bundles that appear much stretched and aligned on the same plane as the epidermis.

3. Current methodologies of wound diagnosis

In clinical practice wound diagnosis is carried out by clinical signs based on the practice and expertise of the physician. For more quantitative and qualitative assessment, histochemical biopsies are employed. Some methodologies commonly used by the clinicians for wound diagnoses are as follows:

(a) *Use of clinical signs:* The clinical signs of infection are erythema, edema, heat, pain, foul odor, and wound breakdown [4]. A physician has to make a firm decision of a wound status on the basis of his or her experience. However, there are several intrinsic limitations to diagnosing a wound through these techniques as all of them are non-quantitative.

(b) *Clinical biopsies:* A biopsy is a medical examination commonly performed by a pathologist involving slice of tissue sections from a diseased or inflamed body part for insights into possible cancerous and inflammatory conditions. It is the medical removal of tissue from a living subject, which is processed into thin slices stained for observation under a microscope or analyzed by biochemical means. This kind of diagnosis has the disadvantage that the method can enlarge the wound. Moreover the time required from biopsy collection to analysis can influence the data and interfere with the wound [5, 26].

(c) *Needle aspiration:* It is a diagnostic procedure used to investigate superficial inflammation, lumps, or masses. In this technique, a thin, hollow needle is inserted into the mass and a portion of the tissue is recovered. The recovered tissue with the cells is stained and examined under a microscope. Needle aspiration biopsies are minor surgical procedures and safe. In spite of being considered as the next best method for microbiological culturing of abscesses and closed wounds, there is a risk, because the biopsy is very small (only a few cells), that the problematic cells may be missed, resulting in a false-negative result [5, 27] that prohibits a definitive diagnosis.

Recently noninvasive approaches have been brought in for assessing skin lesions that include magnetic resonance, ultrasound, and photoacoustic and optical techniques with which intravital imaging of the alterations or aberrations in the skin below the surface has been materialized [28]. Among them optical microscopic techniques provide cost effective and wider range of applications of skin tissue imaging.

4. Optical techniques used in skin observations

Optical imaging techniques are based on the principles of light and tissue interaction for collecting information that is further analyzed to reconstruct an image of the respective tissue section. Depending on the nature of interactions, such as scattering, absorption, or fluorescence, various information can be extracted to reveal anomalies in the tissue sections. The physiological events associated with such structural anomalies also determine the choice of optical modality needed to address the problem noninvasively. In a few excellent reviews,

various optical approaches in skin imaging are listed and discussed depending on the skin conditions [28–31].

Optical modalities are comparatively advantageous for their low-cost, easy to use, non-ionizing, mostly noninvasive, and non-contacting attributes. Some of the optical methodologies can provide 3D imaging capability by optical sectioning with high resolution [32–35]. Optical techniques may also be useful in real-time functional imaging regarding skin physiology [36]. Additionally, most of the skin optical imaging techniques use near-infrared (NIR) or infrared (IR) wavelengths, which are less absorbed in tissue, hence penetrating deeper, enabling the imaging of the whole skin layer [37–39]. Most common optical imaging modalities include LDI, tissue spectral imaging (TSI), and OCT, which are useful in imaging macro-masses in skin (macro-imaging modalities). Optical techniques that are useful in imaging at molecular domain or micro contrasts (micro-optical modalities) are RCLM, Raman spectro-microscopy, and laser scanning fluorescence and SHG microscopy. In this section, we are going to discuss the recent advancements in optical techniques that have been applied to evaluate skin wound-related problems noninvasively or hold potential in this regard. The following is separated into two subsections: the macro-optical modalities and micro-optical modalities.

4.1. Macro-optical imaging modalities

4.1.1. Dermoscopy

Dermoscopy or dermatoscopy, also known as epiluminescence microscopy, is the most common basic handheld magnifying tool that aids in first-line optical observation of morphological abnormalities. Recent dermoscopes use polarized light to illuminate the tissue section to visualize horizontal morphological features that are not visible to naked eye [40]. Dermoscopy has been useful in qualitative visualization of skin-related abnormalities such as rosacea [41], diagnosis of hair and scalp diseases [41–43], diagnosis of warts caused by human papillomavirus [44], and determination of the surgical margin of hard to define skin cancers [41].

This method has been widely used in observing skin lesions based on the presence of certain architectural characteristics of the lesion, which provide promising possibilities in skin wound healing study, mainly in collagen regeneration during wound remodeling phase [45]. A dermoscope is easy to use and represents a relatively low-cost first-line diagnostic tool for skin-related issues; however it is not quantitative and requires expertise and experience to have fair diagnostic judgment [46]. Its resolution is only enough to see small lumps and lesions in the skin. Additionally, no functional information can be gathered with this technique. Commercial dermoscopes are available in the market for quite a few time. Companies such as Optilia, WelchAllyn, CALIBER, HYMED, and FotoFinder are manufacturing dermoscopy products of various specifications and models with attached digital cameras to it that are capable of videography also.

4.1.2. Laser Doppler imaging

In LDI, laser light is used to illuminate the tissue section and the backscattered as well as reflected light is collected to image any moving object within the tissue section. With this technique blood flow through superficial skin layer can be calculated based on the Doppler shift introduced by moving blood cells [47, 48]. It is useful in measuring blood perfusion unit [48], which can be applied in extracting useful functional information to assess angiogenesis and endothelial functioning during wound healing [49].

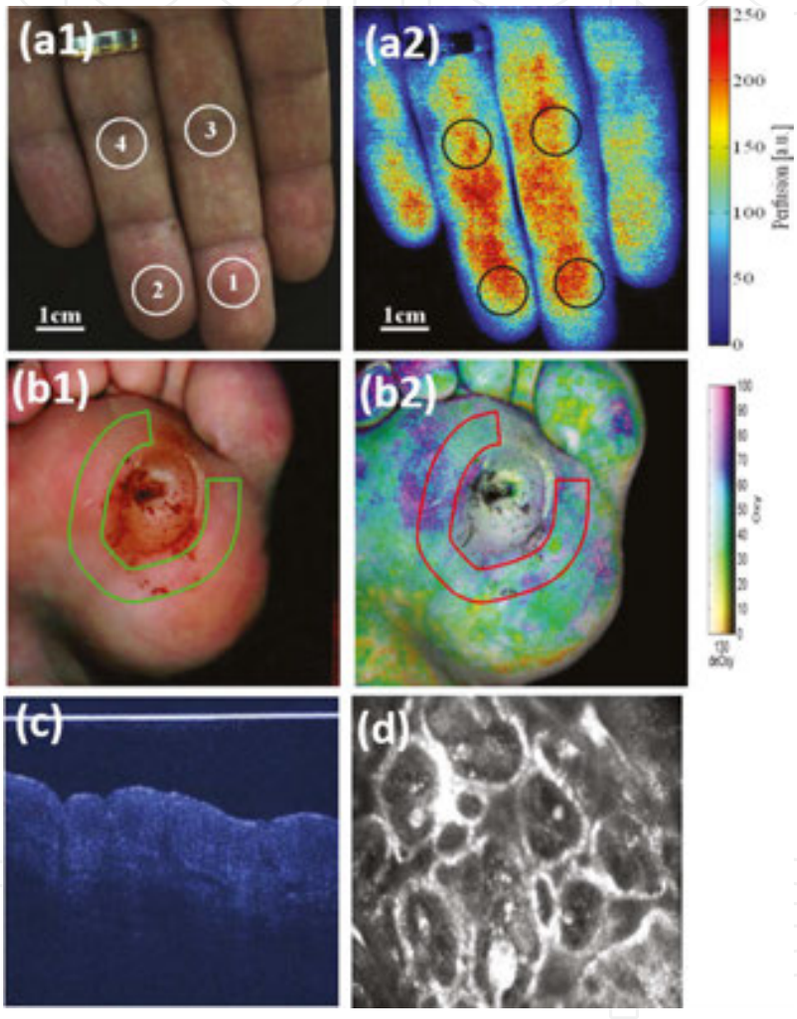

Figure 2. (a1) Visible color image of fingertips and (a2) color-coded blood perfusion map [51]. (b1) Visible and (b2) hyperspectral image of a healing diabetic foot ulcer taken with the HTOM system. HTOM values are 60, 53, and 53% for oxy, deoxy, and StO_2, respectively [57]. (c) OCT signals using a super luminescent NIR diode [25] and (d) reflectance confocal microscopy image at wavelength 830 nm of a human nevus detected by VivaScope [25].

LDI is a low-cost, easy to use noninvasive imaging modality compatible with classical medical instrumentation, where discomfort and risk to patients are minimal. A typical LDI system has a resolution of about 2 mm × 2 mm with an average imaging depth of 200–240 μm [50, 51]. **Figure 2(a1)** and **(a2)** depicts a representative comparison of visible **(a1)** and color-coded blood

perfusion map **(a2)** [51]. LDI has been reported to be used in imaging microcirculation in burned skin and monitoring blood flow recovery in a skin flap during reconstructive surgery demonstrating its potential for clinical wound assessment applications [47]. There are several other reports of burn wound depth and healing assessment with LDIs in clinical and research settings both on human and animals [50, 52, 53].

Commercial instruments based on the principle of LDI are made available by company such as Moor Instruments for skin perfusion assessments. The moorLDI2-IR laser Doppler blood flow imager can image an area up to 50 cm × 50 cm in one scan in less than 5 minutes. Due to the large area scanning possibility, this method has been very useful in burn wound depth and healing assessment based on angiogenesis.

The main disadvantage of this technique is its limited application only in observation of blood flow, similar to that of laser spackle imaging. It is unable to provide any other functional as well as structural information of skin integrities. The poor resolution in millimeter range is another major limitation of this technique in comparison with other optical techniques. Additionally, the use of visible light illumination in LDI limits its applicability in deep dermal wound assessments.

4.1.3. Tissue spectral imaging

Tissue spectral imaging (TSI) is a technique where a tissue of interest is illuminated by a broadband light and collects the reflected or diffused light through selective narrowband filters in front of the detection unit. This technique thus yields several images of specific wavelengths on the same area, providing quantitative measures of the absorbers or scatterers present [54]. Skin has several chromophores such as hemoglobin, melanin, collagen, and other biomolecules which absorb or scatter light and are responsible for skin physiology.

Diffused multispectral imaging (DMSI) is a type of TSI in which the diffused light through a tissue section was collected with a narrow band-pass filter in front of the detection unit. Based on peak absorption, specific wavelengths were chosen to reconstruct an image that can provide physiological information. It is a widely used technique in imaging hemoglobin as it can discriminate oxygenated and deoxygenated hemoglobin by their spectral signature [28]. Most of the DMSI uses NRI wavelength (700–1,100 nm) for quantitative spectroscopic analysis of structural and chemical integrity of cutaneous tissue, especially oxygen saturation, hemoglobin content, and water content. Careful assessment of the absorption spectra can be applied to monitor the wound severity and healing. Reports at preclinical setting have demonstrated the potential of this technique in differentiating superficial-, intermediate-, deep-, and full-thickness burn wounds based on measurement of water content, oxygen saturation, and total hemoglobin concentration [55, 56]. It has also been found useful in diabetic ulcer assessment and predicting diabetic wound healing as well as differentiating diabetic wounds from nondiabetic wounds [37, 38].

Hyperspectral imaging (HSI) is an effective technique that can capture and map detailed spectroscopic information for every pixel in an image. A single pixel in a hyperspectral image provides information in two-special dimension and one spectral dimension creating a 3D data

cube [30]. HSI has been reported to be used in diagnosing diabetic foot ulcers [57, 58] and burn wound edemas [59] where cutaneous tissue oxygenation is observed by assessing oxy- and deoxy-hemoglobin as spectroscopic contrasts. Based on HSI of hemoglobin oxygenation in wound site and areas adjacent to ulcer, wound healing index has been developed [58]. HSI using broadband visible light-emitting diodes has been reported to generate tissue anatomical oxygen map that predicts the risk of diabetic foot ulceration in pre-ulceration tissue [60]. **Figure 2(b1)** and **(b2)** depicts a representative comparison of visible and hyperspectral image of a healing diabetic foot ulcer taken with the hyperspectral tissue oxygenation mapping (HTOM) system [57].

Spectrophotometric intracutaneousanalysis (SIAscope) is a kind of TSI technique based on back-reflected light of wavelength within the range of 400–1000 nm. It is a portable, fast device that predicts burn wound depth by creating a quantitative map of specific chromophores [61]. TSI based on reflectance has also found to have potential in assessing hematomas on the basis of hemoglobin destruction quantification that can determine the age of hematomas in vivo [62]. This information can also be crucial in identifying the layer of skin that sustains the hematoma [63].

Orthogonal polarization spectral imaging (OPSI) uses linearly polarized light to illuminate the skin tissue and collect the emergent depolarized light scattered by the skin components through an analyzer positioned orthogonal to the plane of illumination light polarization [64]. By analyzing the depolarized light, hemoglobin in microcirculation can be visualized to quantify the microvasculature during cutaneous wound healing [65–68].

Thermographic spectroscopy is a spectroscopic imaging technique based on the principle that all the objects including the skin have a heat signature that radiates in IR wavelength. This emission can be detected by using appropriate detector and construct color-coded images that correlate the relative temperature of the specific skin area [69–71]. Usually superficial burn wounds are warmer than uninjured skin due to increased inflammatory processes while deeper burns are cooler than uninjured skin due to structural damage to the vasculature. By using this basic principle, burn wound depth and healing progress over time can be predicted [71, 72].

A number of modalities of TSI have been commercialized by companies such as HySpex and Specim's AisaFENIX. The TSI technique can provide better resolution than LDI, typically up to 0.4–1 μm. Being a wide-field imaging technique, TSI is unable to provide a detailed 2D sectioned image with better resolution; rather it only can provide a molecular map in a certain area. It also suffers from scattering blur and diffraction limitations and has low penetration depth. Additionally, to gather a meaningful spectral information, it requires enough photon information which makes it a relatively slow method. Even with these limitations, this technique holds potential for functional imaging of blood clotting, blood flow during wound inflammation phase, and angiogenesis during superficial skin wounds. Recent advancements in computational methodologies have shown great promises in real-time quantitative functional imaging with improved resolution [54].

4.1.4. Optical coherence tomography (OCT)

OCT is a technique that captures 3D images of a tissue. OCT uses reflected light from tissue to construct cross-sectional images from deeper part of the skin. Most common OCTs use IR illumination, which after scattering from tissue is superimposed with a reference light to generate an interferometric pattern that provides high-resolution 3D depth information by scanning the tissue section in all directions [73–76].

OCT has been an established imaging modality in medical diagnosis and research field. Although it is most popularly used in ophthalmology [77], it has also gripped its root in dermatology [78] study such as keratosis [79], skin cancers [80], skin fibrosis [81], and wound healing. Other than that, it has also been reported to be used in other dermatological problems such as inflammatory diseases and parasitic infection and those of the nails [75, 76]. Recent advancement in OCT allows use of polarized light to image extracellular matrix and other connective tissues in the skin layer that are polarization sensitive [82, 83]. Reports also suggest use of phase-resolved OCT for imaging blood flow in the skin [84]. There are a few excellent reviews that have listed and discussed various applicable possibilities for OCT in dermatology [83, 85, 86].

In diagnosis of wound healing, there are reports of comparing healing assessment of acute wound [87] and superficial wound caused by bacterial infection on mice by OCT to histological findings [88]. A study had reported quantitative evaluation of healing kinetics at real time after fractional laser therapy by OCT demonstrating excellent correlation with findings from histopathological observations [89]. In an in vivo study, OCT has effectively evaluated the various stages of wound healing in 12-day long healing process recognized by re-epithelialization in the early stage, followed by thickening of the epithelial layer around 10th day and formation of scar tissue composed of extracellular matrix along with thickening of epidermal layer in the final stage [90].

OCT's most promising advantage is its ability of axial sectioning and 3D imaging of a tissue mass. OCT techniques using IR light sources are suitable imaging modalities for deep tissue topographical imaging of skin disfigurement. Although the resolution of OCT is lower compared to CLSM or 2PFM or SHG microscopy, the associated resolution degradation with depth is much smaller. OCT cannot produce images at cellular or fibrous molecular resolution; hence it is incapable of imaging a single-cell structure or fibrous collagen structure in the skin dermis [30]. However, in comparison to other macro-optical methodologies, OCT exhibits better resolution. In fact, with sophisticated design, OCT can also achieve a resolution of few tens of micrometer. OCT was also reported to provide even more detailed structural information of a larger mass of tissue than 2PFM at depth of 2–3 mm while imaging thermally injured wounds [91]. OCT is a useful noninvasive technique that has huge potential for wound healing research and assessment. **Figure 2(c)** represents a typical OCT image [25].

OCT has been commercialized by companies such as Optovue, NinePoint Medical, and Thorlabs; two such models from Thorlabs are Ganymede II IR-OCT system and Telesto series spectral domain OCT systems. These systems are mainly operated in IR domain with line scan rate within the range of 5.5–76 KHz.

4.2. Micro-optical modalities

4.2.1. Raman spectro-microscopy

Microscopic imaging based on Raman vibrational spectroscopic contrast provides a useful noninvasive approach for visualizing skin tissues and the corresponding architecture with molecular specificity. A typical Raman microscope detects vibrational scattering changes introduced by the Raman-active molecules in tissue. Molecules rich in CH2 bonds, such as protein and lipid, are good Raman contrast agents and can be interpreted to visualize structural changes occurring in different skin strata [92–94]. An automated Raman micro-spectrometer in confocal settings was reported to be used to determine water concentrations in hydrated and non-hydrated stratum corneum, showing the capacity of this method [95]. However, spontaneous Raman signal is very weak. The Raman detection can be significantly enhanced by CARS. It can visualize structural fibers such as collagen and elastin that constitutes the human dermis along with subcutaneous layer rich in lipids, due to the high density of CH_2 bonds [96–98]. CARS microscopy is the method of choice for studies that require visualization of fat in tissues, which can very effectively characterize obesity in murine skin in vivo [99]. While imaging superficial tissue layers, CARS can provide strong signal from the fat component of the skin that allow video-rate imaging.

Video-rate CARS imaging can be used for imaging lipid lamellae of the stratum corneum, sebaceous glands, and dermal adipocytes, and the fat-containing cells of the subcutaneous layer with imaging depths of up to several hundred micrometers, promising a potential methodology for noninvasive molecular imaging [97]. Recently CARS has also been used in studying transdermal delivery of retinol in mouse ear, a drug with strong CARS signal that stimulates collagen growth in skin and was located in corneocytes of stratum corneum [100].

König and his group have reported a CARS tomography system for skin imaging suitable for clinical environments that is capable of in vivo histology with subcellular resolution and chemical contrast toward patients suffering from psoriasis and squamous cell carcinoma [101]. Their system also has the potential to be used in studying skin wound healing. Although Raman imaging in the form of CARS can provide high-contrast functional imaging with subcellular resolution, it is, however, mostly limited to Raman-active molecules only. In comparison, the Raman scattering cross section is very small which translates to very weak signal intensities, thus requiring very high density of molecules or very long acquisition times in order to acquire a meaningful image.

4.2.2. Laser scanning microscopy techniques:

A commonly used wide-field microscope provides a two-dimensional image, typically in histological observations of biopsies. However it has several drawbacks, including low resolution, low penetration depth, slow imaging rate, and inability to have functional imaging. It delivers poorer image contrast and lacks optical sectioning capability. In contrasts, a laser scanning microscope (LSM) provides a few numbers of platforms for imaging that are improved with respect to all aspects mentioned above. Among them confocal microscopy in linear domain and two-photon fluorescence microscopy (2PFM) and SHG in nonlinear domain

are most prominent. Confocal laser scanning microscopy (CLSM) has several advantages over traditional microscopy, including faster data acquisition, optical sectioning of cells and tissues for 3D imaging, and significantly improved spatial resolution [39, 102, 103]. The pioneering work of Minsky, in the year 1957, initiated the development and the first commercialized CLSM was realized in 1987 [104]. However, CLSM has a relatively lower penetration depth compared to MPM, due to the shorter wavelength used. Single-photon confocal microscopy obtains an image section at the expense of photon efficiency, attributing to the spatial filtering pinhole [39, 105, 106]. The overexposure would cause photo bleaching of the sample. As a result, only highly photostable fluorophores work well with this technique. In comparison, MPM uses IR excitation which reduces photo bleaching in a confined way and allows imaging depths of up to ~2 mm. The nonlinear effect forms a virtual pinhole and saves the trouble of precision alignment needed for a physical pinhole [39, 106].

4.2.2.1. Reflectance confocal laser scanning microscopy (RCLSM)

In RCLSM, a pinhole at the confocal image plane eliminates out-of-focus signal to realize optical sectioning for 3D imaging. It uses a focused laser beam for excitation and forms the image by point to point scanning, usually by a pair of computer-controlled galvano mirrors [32, 33]. The reflected light signal is collected by a photo detector after the pinhole. The reflected signal is de-scanned by the same pair of galvano mirrors so the alignment of pinhole is straightforward [107]. The configuration is widely used in commercially available confocal microscopes for skin imaging [33, 107]. It has also been used for assessing and monitoring cutaneous wound healing by evaluating the cellular and morphological parameters of wound bed and wound margins noninvasively over the course of healing [102]. In the reported study, patients with chronic leg ulcers and skin cancers receiving split skin graft were evaluated against healthy individuals, in which various physiological signatures of wound healings at different phases were documented. For example, appearance of inflammatory cells in the epidermis during the early stage of wound healing, proliferative keratinocytes and their migration during granulation and re-epithelialization phases, and the networks of connective tissues during remodeling phases were observed with reflectance CLSM [102].

A commercially available CLSM in reflectance mode is VivaScope®1500 that has planar and axial resolution of 1.25 and 5.0μm, respectively, with an imaging depth up to 200 μm. Its image acquisition speed of 9 frames per second allows real-time videography of wound healing. **Figure 2(d)** represents a reflectance confocal microscopy image by detecting backscattered 830 nm light from a human nevus with the system [25].

Although these instruments are widely used, they are limited to surface imaging only. Therefore, they are not suitable for evaluating deep dermal wounds. Nevertheless, they can image wound margins, which may provide crucial semiquantitative information regarding wound healing with a resolution comparable to that of histological analysis [30]. The reflection contrast-based CLSM is frequently used for structural imaging but is incapable of molecular functional imaging. A typical CLSM has much improved resolution and faster scanning rate than OCT. However, it may be limited by photo bleaching and diffraction blurring when compared to multiphoton techniques.

4.2.2.2. Confocal fluorescence microscopy

Confocal fluorescence microscopy is a technique that allows imaging of living tissue by collecting fluorescence emission from the chromophores present in the tissue. In single-photon fluorescence imaging, a fluorophore absorbs a single photon to be excited into a higher energy state before emitting the fluorescence, and comes down to original lower energy state. The simplest fluorescence imaging instrumentation uses a laser to illuminate the skin at a specific excitation wavelength and collects the filtered fluorescence emission with a detector bearing an optical filter in front of it.

Fluorescence imaging can be done with either staining the tissue by exogenous fluorescent materials or imaging endogenous fluorescence from skin's natural fluorophores. Indocyanine green (ICG) is one commonly used exogenous fluorescence dye that can be located in systemic circulation, which allows the imaging of vascularization and the determination of imaging depth [108]. This technique has been shown to quantitatively measure blood flow in the cutaneous wound that is well correlated with the histological assessment of burn depth [108]. As mentioned in Section 2, endogenous fluorophores, NADH, FAD, and collagen are all important markers in wound healing processes that can be used for wound diagnosis [36, 109].

Along with NADH and FAD, collagen is another abundant molecule present in the skin dermis that is autofluorescing. It can serve as a marker upon exposure to the 325 nm He-Cd laser treatment (~2 J/cm^2) during skin tissue regeneration, as shown in mouse model by detecting the collagen autofluorescence intensity [110]. In another comparative ex vivo and in vivo study of wound granulation by the same group, normalized NADH/collagen autofluorescence intensity was used to assess collagen deposition during healing [111].

Confocal fluorescence microscopy can provide real-time functional imaging of cells and tissues with improved resolutions. However single-photon imaging may be limited by photo bleaching and low penetration depth. Alternatively, MPF imaging would improve photo stability with deeper penetration.

4.2.2.3. Multiphoton microscopy (MPM)

In multiphoton imaging a simple confocal laser scanning microscope is used with an ultrafast NIR laser source. The pinhole is usually removed and the detection unit is modified with specialized filters. Multiphoton laser technique greatly improves resolution and penetration depth than macro-optical modalities. Its optical sectioning ability does not require a pinhole, which reduces alignment difficulty and the volume of photo bleaching. Additionally, the NIR excitation wavelengths are shown to extend the limit of deep tissue imaging up to 2 mm.

In tissue imaging, commonly used multiphoton techniques are 2PFM and SHG imaging. In 2PFM, the fluorophores absorb two photons simultaneously to be excited to a higher energy real state before emitting the fluorescence, while in SHG, the two photons of the same energy would combine to form a new photon of twice the energy of the incident photon. Biomolecules such as collagen and muscle myosin with noncentrosymmetric molecular structures have the ability to generate SHG signal [8, 112–114]. Skin can be imaged with both fluorescence and SHG contrasts simultaneously with the help of a laser scanning MPM [36, 115]. Zoumie et al.

in their study of a tissue model have described spectrally resolved imaging of different parts of the skin layers by a combined 2PFM and SHG setup [115]. They detected fluorescence from cellular NADH and SHG from collagen. The study of wound healing with fluorescence and SHG is discussed in the following paragraphs.

Cellular NADH autofluorescence in two-photon modality has been used as marker for morphological characterization of epithelia both in vivo [116–118] and ex vivo [119] for animal and human tissues as well as fresh biopsies [120]. It enables optical microscopic imaging being equivalent to histochemical analysis. With the help of 2PFM imaging, various epidermal layers of in vivo skin were discriminated at subcellular spatial resolution based on cellular morphological features [31]. Additionally, the time-correlated single-photon counting technique in conjunction with 2PFM has made functional imaging possible by measuring the lifetime of fluorophores. This technique, termed as fluorescence lifetime imaging (FLIM), is very effective in determining real-time cellular metabolic activity in vivo by measuring the fluorescence lifetime decay of NADH. Cells located in the basal layer exhibit the strongest metabolic activities, while epidermal surface layered cells are found to have lower metabolic activities. FLIM has demonstrated its capacity in characterizing epithelial tissue involved in wound healing and other pathological conditions [31].

NADH, being a metabolic coenzyme, is associated with the cellular metabolic activities through the electron transport chain (ETC) of oxidative phosphorylation. NADH has two functional forms, free and bound. During the process of energy generation, free NADH is bound to mitochondrial membrane proteins [36]. Although the fluorescence emission spectra of both free and bound forms of NADH fall in a very narrow band, their fluorescence lifetimes are well separated. When NADH binds to a protein, its lifetime increases from ~0.4 to ~2.5 ns [121–123]. Therefore by evaluating the contribution of free and bound states to the combined double exponential lifetime, the relative concentrations of individual states can be predicted. In simple words, a cell with higher metabolic activity has a higher concentration of bound NADH than a cell with lower metabolic activity. In addition to that the ratio of bound form NADH to bound form of FAD, termed as cellular redox ratio, can also be a marker for relative metabolic activity determination [124].

The cellular metabolic parameters are viable markers for evaluating wound healing. We have demonstrated on live rat models that the cellular metabolic rate correlates well with wound healing phases [36]. In the study, artificially created incisional wound by punch biopsy was used to evaluate the wound healing from the day of wound formation to scar formation in a 20-day healing course with 2PFM and SHG microscopy. The relative metabolic activities of cells involved in the process of wound healing as time progresses were evaluated by the NADH bound to free ratio, while the changes in collagen concentration are correlated with SHG intensity. These findings suggest the metabolic activities at the wounded sites increase during inflammatory and granulation phases and gradually decrease as wound heals (**Figure 3(b)**). Interestingly, in the beginning of healing, SHG intensity decreases (or collagen concentration), indicating the degradation of collagen in the dermal layer during cell migration. Once new collagens were formed, SHG signal started to increase gradually (**Figure 3(c)**). In general, wounds heal gradually from the edge toward the center; hence the metabolic activities are

IntechOpen

Figure 3. (a) Representative color-coded NADH free/bound (a_1/a_2) lifetime ratio images (left column) and gray-scale SHG intensity images (right column) of collagen regeneration during wound healing [132]. (b) Scatter plot of NADH a_1/a_2 distribution peak value with healing progress both at the center and edge, averaged over 15 wounds at each day of wound observation. The ratio NADH a_1/a_2 is inversely proportional to metabolic activity of cells. Two-side Student's *t*-test evaluated significant differences of NADH a_1/a_2 values at the center from normal skin that are indicated by *, $P > 0.05$; **, $0.05 > P > 0.001$; and ***, $P < 0.001$. The significant differences of a_1/a_2 values at the edge from the normal skin are designated as #, $P > 0.05$; ##, $0.05 > P > 0.001$; and ###, $P < 0.001$ [132]. (c) Scatter plot of normalized SHG intensity with respect to the maximum intensity observed at the edge on day 20. The changes in SHG intensity elucidate the relative degradation and regeneration of collagen at the center and the edge in the course of wound healing. Two-side Student's *t*-test evaluated significant differences of SHG intensity at center from normal skin that are indicated by *, $P > 0.05$; **, $0.05 > P > 0.001$; and ***, $P < 0.001$ for center. The significant differences of SHG intensity values at edge from normal skin are designated as #, $P > 0.05$; ##, $0.05 > P > 0.001$; and ###, $P < 0.001$. *P* value less than 0.05 was considered significant [132].

higher at the edge in the early stages of wound healing, marked by the higher bound to free NADH ratio in lifetime measurement. However, in the proliferative phase the center has higher metabolic activity than the edge since the edge has entered the remodeling phase, in which cell activity decreases and collagen is deposited to fill the wound gap, marked by the increase of SHG intensity. Following the proliferative phase, the whole wound is filled with granulation tissues, mainly collagen, and the cellular metabolism decreases gradually. The wound then heals into a scar, composed of connective tissues marked with higher SHG signal intensity than that from a normal tissue. The lack of cells in scar tissue reduces the need for blood influx, which results in removal of blood vessels by apoptosis and leaves a scar tissue characterized by lower metabolic activity and higher collagen deposition.

The changes of the NADH free to bound ratio (**Figure 3(b)**) and the collagen SHG intensity (**Figure 3(c)**) exhibit as the signature of the various phases in wound healing, which can be used for crucial diagnosis and proper treatment. With the simultaneous measurements of 2PFM and SHG, a correlation between cellular metabolic activities and collagen regeneration can be observed. In **Figure 3(a)**, the morphological features of cells and their gradual appearance in wound region and structural evolution of collagen in a healing wound, acquired by 2PFM and SHG, respectively, are demonstrated. The disordered collagen in normal skin is degraded and more structured collagens are deposited in the process of scar formation as shown in **Figure 3(a)**.

Similar results have also been reproduced by other researchers using combined SHG and 2PFM imaging, where disorganized collagen in fibrin clots and inflammatory cells involved during the early stage of wound healing are distinguished from more organized and aligned collagens in regenerated new skin [125].

SHG is also used in showing the orientation of collagen fibers and their structural changes in the healthy tissues of human dermis [126–129] as well as in in vivo tissue constructs [130]. The efficiency of SHG signal is highly sensitive to the collagen orientation when the incident light is polarized. Along with intensity measurements, polarization-resolved SHG provides information on collagen alignment and orientation during regeneration, which is correlated to wound closure and the way scar tissue forms [131].

Polarization-resolved SHG indicates that collagens are more organized and fibrillary during the proliferative phase, to aid in wound closure when the margins are pulled together by them [132]. In this way, the anisotropic variation of collagen during wound healing can be monitored by collecting the parallel (I_{par}) and the perpendicular (I_{perp}) components of the polarized SHG signals with respect to the incident polarization. **Figure 4** demonstrates representative I_{par} (first row) and I_{par} (second row) polarization-resolved SHG intensity images from biopsy samples taken after discrete days of wound formation along with corresponding anisotropy images (third row) defined by $(I_{par}\text{-}I_{perp})/(I_{par}+2I_{perp})$. Anisotropy value equal to 0 corresponds to complete random arrangement of the scatterers, and if it is equal to 1, it corresponds to having a well-aligned, well-structured scattered system [132, 133]. Anisotropic observation of ex vivo rat skin biopsies has revealed maximum anisotropy value of collagen during wound contraction and closure. When the wound gap is filled with matured collagen, the anisotropy decreases gradually [132].

Figure 4. Representative polarization-resolved SHG intensity images of wound biopsy samples taken at different healing stages. The first row depicts the images with the parallel (I_{par}) component. The second row depicts the images with the perpendicular (I_{par}) component. The third row depicts the corresponding anisotropy images defined by (I_{par}-I_{perp})/(I_{par} +2I_{perp}) [132].

In clinical setting, multiphoton imaging of human epidermis and upper dermis has been achived by commercial system such as DermaInspect™ that is able to scan an area of 350 μm×350 μm with special resolution of 1 μm in lateral and 2 μm in axial directions [25]. The system provide non-invasive in vivo optical biopsies of skin at subcellular resolution by detecting autofluorescence from biomolecules such as NADH, flavins, porphyrins, elastin and melanin and SHG signals from collagens.

5. Conclusion

Wound healing is an important physiological process that follows a certain sequential order. Migration of various cells and the involvement of certain molecules at the wound site characterize the various phases during healing progression. Detailed quantitative and qualitative information of these components at a specific time provides critical insights on wound healing. Optical methodologies are versatile and include techniques that can gather a wide variety of information on multiple components noninvasively, which presents tremendous future prospects in terms of clinical implications. The available modalities present enormous potentials to supplement clinical assessment and to aid research in the field of cutaneous healing and skin tissue regeneration.

The versatile optical modalities discussed in this chapter have their own significance in assessing specific wound-related problems. Some modalities are simple and easy to operate, which provide relatively low-cost first-line diagnosis. More complex techniques can provide better resolution and sophisticated structural information. By judicially combining various contrasts from the skin components, these optical techniques can address a wide variety of skin wound-related issues. These can include observations of subsurface morphological features using dermascope, blood flow using LDI, molecular and functional signatures using TSI, structural revelation using OCT, RCLM and SHG microscopy, or molecular identification with Raman and fluorescence imaging. Each technique would provide unique yet complimentary information.

Multimodal MPM presents the most sophisticated approach for quick, qualitative, and quantitative skin wound healing study as it integrates multiple contrast mechanisms for imaging the skin. Specifically, 2PFM and SHG are favorable in wound assessment for their high-resolution, better penetration depth, optically sectioned 3D imaging with the provision of structural and real-time molecular functional signature.

Emerging super resolution imaging based on saturation excitation (SAX) of scattering from metallic nanoparticles may extend the possibilities of super resolving the skin abnormalities [134]. Ointments and sunscreen lotion could effectively carry the nanoparticles into skin epidermis to facilitate the new optical techniques. With the ongoing rapid advancements in photonics and imaging, one can expect new and novel techniques will find unprecedented and enlightening applications in dermatology in the coming future.

Author details

Gitanjal Deka[1*], Shi-Wei Chu[1] and Fu-Jen Kao[2]

*Address all correspondence to: gitanjal@yahoo.com

1 Department of Physics, National Taiwan University, Taipei, Taiwan

2 Institute of Biophotonics, National Yang Ming University, Taipei, Taiwan

References

[1] H. Brem, and M. Tomic-Canic, "Cellular and molecular basis of wound healing in diabetes," J. Clin. Invest. 117, 1219-1222 (2007).

[2] M. Peck, J. Molnar, and D. Swart, "A global plan for burn prevention and care," Bull. World. Health. Organ. 87, 802-803 (2009).

[3] P. Martin, "Wound healing--aiming for perfect skin regeneration," Science 276, 75-81 (1997).

[4] S. E. Gardner et al., "A tool to assess clinical signs and symptoms of localized infection in chronic wounds: development and reliability," Ostomy. Wound Manag. 47, 40-47 (2001).

[5] G. Dow et al., "Infection in chronic wounds: controversies in diagnosis and treatment," Ostomy. Wound Manag. 45, 23-40 (1999).

[6] T. Y. Buryakina, P.-T. Su, W.-J Syu, C. A. Chang, H.-F. Fan, and F.-J. Kao, "Metabolism of HeLa cells revealed through autofluorescence lifetime upon infection with entero-hemorrhagic *Escherichia coli*" J. Biomed. Opt. 17, 101503 (2012).

[7] B. Banerjee, T. Renkoski, L. R. Graves, N. S. Rial, V. L. Tsikitis, V. Nfonsam, J. Pugh, P. Tiwari, H. Gavini, and U. Utzinger, "Tryptophan autofluorescence imaging of neoplasms of the human colon," J. Biomed. Opt. 17, 016003 (2012).

[8] W. R. Zipfel, R. M. Williams, R. Christie, A. Y. Nikitin, B. T. Hyman, and W. W. Webb, "Live tissue intrinsic emission microscopy using multiphoton-excited native fluorescence and second harmonic generation," Proc. Natl. Acad. Sci. U. S. A. 100, 7075-7080 (2003).

[9] X. Jiang, J. Zhong, Y. Liu, H. Yu, S. Zhuo, and J. Chen, "Two-photon fluorescence and second-harmonic generation imaging of collagen in human tissue based on multiphoton microscopy," Scanning 33, 53-56 (2011).

[10] W. Denk, J. H. Strickler, and W. W. Webb, "Two-photon laser scanning fluorescence microscopy," Science 248, 73-76 (1990).

[11] P. T. So, C. Y. Dong, B. R. Masters, and K. M. Berland, "Two-photon excitation fluorescence microscopy," Annu. Rev. Biomed. Eng. 2, 399-429 (2000).

[12] Y. Lee, and K. Hwang, "Skin thickness of Korean adults," Surg. Radiol. Anat. 24, 183-189 (2002).

[13] L. A. Baden, "Surgical Anatomy of the Skin," Arch. Dermatol. 125, 719-719 (1989).

[14] G. C. Troy, "An overview of hemostasis," Vet. Clin. North Am. Small Anim. Pract. 18, 5-20 (1988).

[15] T. A. Springer, "Biology and physics of von Willebrand factor concatamers," J. Thromb.Haemost. 9, 130-143 (2011).

[16] H. P. Lorenz, and M. T. Longaker, "Wounds: biology, pathology, and management," in Essential Practice of Surgery (Springer, 2003), pp. 77-88.

[17] F. H. Epstein, A. J. Singer, and R. A. Clark, "Cutaneous wound healing," N. Engl. J. Med. 341, 738-746 (1999).

[18] S. A. Eming, T. Krieg, and J. M. Davidson, "Inflammation in wound repair: molecular and cellular mechanisms," J. Invest. Dermatol. 127, 514-525 (2007).

[19] K. S. Midwood, L. V. Williams, and J. E. Schwarzbauer, "Tissue repair and the dynamics of the extracellular matrix," Int. J. Biochem. Cell Biol. 36, 1031-1037 (2004).

[20] R. F. Diegelmann, and M. C. Evans, "Wound healing: an overview of acute, fibrotic and delayed healing," Front. Biosci. 9, 283-289 (2004).

[21] D. G. Greenhalgh, "The role of apoptosis in wound healing," Int. J. Biochem. Cell Biol. 30, 1019-1030 (1998).

[22] R. O'leary, E. Wood, and P. Guillou, "Pathological scarring: strategic interventions," Eur. J. Surg. 168, 523-534 (2002).

[23] A. Desmoulière, C. Chaponnier, and G. Gabbiani, "Tissue repair, contraction, and the myofibroblast," Wound. Repair. Regen. 13, 7-12 (2005).

[24] T.-L. Tuan, and L. S. Nichter, "The molecular basis of keloid and hypertrophic scar formation," Mol. Med. Today. 4, 19-24 (1998).

[25] K. König, "Clinical multiphoton tomography," J. Biophotonics 1, 13-23 (2008).

[26] L. Brentano, and D. L. Gravens, "A method for the quantitation of bacteria in burn wounds," J. Appl. Microbiol. 15, 670 (1967).

[27] N. S. Levine, R. B. Lindberg, A. D. Mason JR, and B. A. Pruitt JR, "The quantitative swab culture and smear: A quick, simple method for determining the number of viable aerobic bacteria on open wounds," J. Trauma. Acute. Care. Surg. 16, 89-94 (1976).

[28] B. Dasgeb, J. Kainerstorfer, D. Mehregan, A. Van Vreede, and A. Gandjbakhche, "An introduction to primary skin imaging," Int. J. Dermatol. 52, 1319-1330 (2013).

[29] D. W. Paul, P. Ghassemi, J. C. Ramella-Roman, N. J. Prindeze, L. T. Moffatt, A. Alkhalil, and J. W. Shupp, "Noninvasive imaging technologies for cutaneous wound assessment: a review," Wound. Repair. Regen. 23, 149-162 (2015).

[30] H. Albert, "A survey of optical imaging techniques for assessing wound healing," Int. J. Intell. Control Syst. 17, 79-85 (2012).

[31] R. Cicchi, D. Kapsokalyvas, and F. S. Pavone, "Clinical nonlinear laser imaging of human skin: a review," BioMed Res. Int. 2014, 903589 (2014).

[32] S. Paddock, T. Fellers, and M. Davidson, *Confocal Microscopy*, Humana Press, Spinger, New York (2001).

[33] M. Rajadhyaksha, S. González, J. M. Zavislan, R. R. Anderson, and R. H. Webb, "In vivo confocal scanning laser microscopy of human skin II: advances in instrumentation and comparison with histology," J. Invest. Dermatol. 113, 293-303 (1999).

[34] J. Fredrich, "3D imaging of porous media using laser scanning confocal microscopy with application to microscale transport processes," Phys. Chem. Earth. Pt. A 24, 551-561 (1999).

[35] J. Lawrence, D. Korber, B. Hoyle, J. Costerton, and D. Caldwell, "Optical sectioning of microbial biofilms," J. Bacteriol. 173, 6558-6567 (1991).

[36] G. Deka, W.-W. Wu, and F.-J. Kao, "In vivo wound healing diagnosis with second harmonic and fluorescence lifetime imaging," J. Biomed. Opt. 18, 061222 (2013).

[37] M. S. Weingarten, E. Papazoglou, L. Zubkov, L. Zhu, G. Vorona, and A. Walchack, "Measurement of optical properties to quantify healing of chronic diabetic wounds," Wound. Repair. Regen. 14, 364-370 (2006).

[38] E. S. Papazoglou, L. Zubkov, L. Zhu, M. S. Weingarten, S. Tyagi, and K. Pourrezaei, "Monitoring diabetic wound healing by NIR spectroscopy," in Conf. Proc. IEEE. Eng. Med. Biol. Soc. (IEEE, 2005) Shanghai, China, pp. 6662-6664.

[39] A. Diaspro, *Confocal and Two-photon Microscopy: Foundations, Applications and Advances*, Wiley-VCH; New York, (2001).

[40] E. Ruocco, G. Argenziano, G. Pellacani, and S. Seidenari, "Noninvasive imaging of skin tumors," Dermatol. Surg. 30, 301-310 (2004).

[41] G. Micali, F. Lacarrubba, D. Massimino, and R. A. Schwartz, "Dermatoscopy: alternative uses in daily clinical practice," J. Am. Acad. Dermatol. 64, 1135-1146 (2011).

[42] S. Inui, T. Nakajima, and S. Itami, "Significance of dermoscopy in acute diffuse and total alopecia of the female scalp: review of twenty cases," Dermatology 217, 333-336 (2008).

[43] M. Wu, S. Hu, and C. Hsu, "Use of non-contact dermatoscopy in the diagnosis of scabies," Dermatol. Sinica. 26, 112-114 (2008).

[44] E.-M. De Villiers, C. Fauquet, T. R. Broker, H.-U. Bernard, and H. zur Hausen, "Classification of papillomaviruses," Virology 324, 17-27 (2004).

[45] G. Argenziano, H. P. Soyer, S. Chimenti, R. Talamini, R. Corona, F. Sera, M. Binder, L. Cerroni, G. De Rosa, and G. Ferrara, "Dermoscopy of pigmented skin lesions: results of a consensus meeting via the Internet," J. Am. Acad. Dermatol. 48, 679-693 (2003).

[46] G. Pagnanelli, H. Soyer, G. Argenziano, R. Talamini, R. Barbati, L. Bianchi, E. Campione, I. Carboni, A. Carrozzo, and M. Chimenti, "Diagnosis of pigmented skin lesions by dermoscopy: web-based training improves diagnostic performance of non-experts," Br. J. Dermatol. 148, 698-702 (2003).

[47] M. Leutenegger, E. Martin-Williams, P. Harbi, T. Thacher, W. Raffoul, M. André, A. Lopez, P. Lasser, and T. Lasser, "Real-time full field laser Doppler imaging," Biomed. Opt. Express 2, 1470-1477 (2011).

[48] K. Wårdell, A. Jakobsson, and G. E. Nilsson, "Laser Doppler perfusion imaging by dynamic light scattering," IEEE Trans Bio-Med Eng 40, 309-316 (1993).

[49] S. Kubli, B. Waeber, A. Dalle-Ave, and F. Feihl, "Reproducibility of laser Doppler imaging of skin blood flow as a tool to assess endothelial function," J. Cardiovasc. Pharmaco. 36, 640-648 (2000).

[50] Z. Niazi, T. Essex, R. Papini, D. Scott, N. McLean, and M. Black, "New laser Doppler scanner, a valuable adjunct in burn depth assessment," Burns 19, 485-489 (1993).

[51] M. Leutenegger, E. Martin-Williams, P. Harbi, T. Thacher, W. Raffoul, M. André, A. Lopez, P. Lasser, and T. Lasser, "Real-time full field laser Doppler imaging," Biomed. Opt. Express 2, 1470-1477 (2011).

[52] S. A. Pape, C. A. Skouras, and P. O. Byrne, "An audit of the use of laser Doppler imaging (LDI) in the assessment of burns of intermediate depth," Burns 27, 233-239 (2001).

[53] E. Droog, W. Steenbergen, and F. Sjöberg, "Measurement of depth of burns by laser Doppler perfusion imaging," Burns 27, 561-568 (2001).

[54] J. M. Kainerstorfer, M. Ehler, F. Amyot, M. Hassan, S. G. Demos, V. Chernomordik, C. K. Hitzenberger, A. H. Gandjbakhche, and J. D. Riley, "Principal component model of multispectral data for near real-time skin chromophore mapping," J. Biomed. Opt. 15, 046007 (2010).

[55] M. G. Sowa, L. Leonardi, J. R. Payette, J. S. Fish, and H. H. Mantsch, "Near infrared spectroscopic assessment of hemodynamic changes in the early post-burn period," Burns 27, 241-249 (2001).

[56] K. M. Cross, L. Leonardi, M. Gomez, J. R. Freisen, M. A. Levasseur, B. J. Schattka, M. G. Sowa, and J. S. Fish, "Noninvasive measurement of edema in partial thickness burn wounds," J. Burn. Care. Res. 30, 807-817 (2009).

[57] A. Nouvong, B. Hoogwerf, E. Mohler, B. Davis, A. Tajaddini, and E. Medenilla, "Evaluation of diabetic foot ulcer healing with hyperspectral imaging of oxyhemoglobin and deoxyhemoglobin," Diabetes care 32, 2056-2061 (2009).

[58] L. Khaodhiar, T. Dinh, K. T. Schomacker, S. V. Panasyuk, J. E. Freeman, R. Lew, T. Vo, A. A. Panasyuk, C. Lima, and J. M. Giurini, "The use of medical hyperspectral technology to evaluate microcirculatory changes in diabetic foot ulcers and to predict clinical outcomes," Diabetes Care 30, 903-910 (2007).

[59] M. A. Calin, S. V. Parasca, R. Savastru, and D. Manea, "Characterization of burns using hyperspectral imaging technique – a preliminary study," Burns 41, 118-124 (2015).

[60] D. Yudovsky, A. Nouvong, K. Schomacker, and L. Pilon, "Assessing diabetic foot ulcer development risk with hyperspectral tissue oximetry," J. Biomed. Opt. 16, 026009 (2011).

[61] H. Tehrani, M. Moncrieff, B. Philp, and P. Dziewulski, "Spectrophotometric intracutaneous analysis: a novel imaging technique in the assessment of acute burn depth," Ann. N Y. Acad. Sci. 61, 437-440 (2008).

[62] V. Hughes, P. Ellis, T. Burt, and N. Langlois, "The practical application of reflectance spectrophotometry for the demonstration of haemoglobin and its degradation in bruises," J. Clin. Pathol. 57, 355-359 (2004).

[63] M. Bohnert, R. Baumgartner, and S. Pollak, "Spectrophotometric evaluation of the colour of intra-and subcutaneous bruises," Int. J. Dermatol. 113, 343-348 (2000).

[64] W. Groner, J. W. Winkelman, A. G. Harris, C. Ince, G. J. Bouma, K. Messmer, and R. G. Nadeau, "Orthogonal polarization spectral imaging: a new method for study of the microcirculation," Nat. Med. 5, 1209-1212 (1999).

[65] S. Langer, F. Born, R. Hatz, P. Biberthaler, and K. Messmer, "Orthogonal polarization spectral imaging versus intravital fluorescent microscopy for microvascular studies in wounds," Ann. N Y. Acad. Sci. 48, 646-653 (2002).

[66] O. Goertz, A. Ring, A. Köhlinger, A. Daigeler, C. Andree, H.-U. Steinau, and S. Langer, "Orthogonal polarization spectral imaging: a tool for assessing burn depths?" Ann. N Y. Acad. Sci. 64, 217-221 (2010).

[67] S. M. Milner, "Predicting early burn wound outcome using orthogonal polarization spectral imaging," Int. J. Dermatol. 41, 715-715 (2002).

[68] S. M. Milner, S. Bhat, S. Gulati, G. Gherardini, C. E. Smith, and R. J. Bick, "Observations on the microcirculation of the human burn wound using orthogonal polarization spectral imaging," Burns 31, 316-319 (2005).

[69] A. Renkielska, A. Nowakowski, M. Kaczmarek, and J. Ruminski, "Burn depths evaluation based on active dynamic IR thermal imaging—a preliminary study," Burns 32, 867-875 (2006).

[70] N. J. Prindeze, P. Fathi, M. J. Mino, N. A. Mauskar, T. E. Travis, D. W. Paul, L. T. Moffatt, and J. W. Shupp, "Examination of the early diagnostic applicability of active dynamic thermography for burn wound depth assessment and concept analysis," J. Burn. Care. Res. 36, 626-635 (2015).

[71] R. N. Lawson, G. Wlodek, and D. Webster, "Thermographic assessment of burns and frostbite," Can. Med. Assoc. J. 84, 1129-1131 (1961).

[72] A. Renkielska, A. Nowakowski, M. Kaczmarek, M. K. Dobke, J. Grudziński, A. Karmolinski, and W. Stojek, "Static thermography revisited—an adjunct method for determining the depth of the burn injury," Burns 31, 768-775 (2005).

[73] A. F. Fercher, "Optical coherence tomography–development, principles, applications," Zeitschrift Med. Phys. 20, 251-276 (2010).

[74] D. Huang, E. A. Swanson, C. P. Lin, J. S. Schuman, W. G. Stinson, W. Chang, M. R. Hee, T. Flotte, K. Gregory, and C. A. Puliafito, "Optical coherence tomography," Science 254, 1178-1181 (1991).

[75] E. Sattler, R. Kästle, and J. Welzel, "Optical coherence tomography in dermatology," J. Biomed. Opt. 18, 061224 (2013).

[76] A. Pagnoni, A. Knuettel, P. Welker, M. Rist, T. Stoudemayer, L. Kolbe, I. Sadiq, and A. Kligman, "Optical coherence tomography in dermatology," Skin. Res. Technol. 5, 83-87 (1999).

[77] L. M. Sakata, J. DeLeon-Ortega, V. Sakata, and C. A. Girkin, "Optical coherence tomography of the retina and optic nerve–a review," Clin. Experiment. Ophthalmol. 37, 90-99 (2009).

[78] S. Chua, "High-Definition Optical Coherence Tomography for the Study of Evolution of a Disease," Dermatol. Bullet. 26, 2-3 (2015).

[79] V. R. Korde, G. T. Bonnema, W. Xu, C. Krishnamurthy, J. Ranger-Moore, K. Saboda, L. D. Slayton, S. J. Salasche, J. A. Warneke, and D. S. Alberts, "Using optical coherence tomography to evaluate skin sun damage and precancer," Lasers Surg. Med. 39, 687-695 (2007).

[80] M. Mogensen, L. Thrane, T. M. Jørgensen, P. E. Andersen, and G. B. Jemec, "OCT imaging of skin cancer and other dermatological diseases," J. Biophotonics 2, 442-451 (2009).

[81] O. Babalola, A. Mamalis, H. Lev-Tov, and J. Jagdeo, "Optical coherence tomography (OCT) of collagen in normal skin and skin fibrosis," Ann. N Y. Acad. Sci. 306, 1-9 (2014).

[82] S. Sakai, M. Yamanari, Y. Lim, N. Nakagawa, and Y. Yasuno, "In vivo evaluation of human skin anisotropy by polarization-sensitive optical coherence tomography," Biomed. Opt. Express 2, 2623-2631 (2011).

[83] M. C. Pierce, J. Strasswimmer, B. H. Park, B. Cense, and J. F. de Boer, "Advances in optical coherence tomography imaging for dermatology," J. Invest. Dermatol. 123, 458-463 (2004).

[84] Y. Zhao, Z. Chen, C. Saxer, S. Xiang, J. F. de Boer, and J. S. Nelson, "Phase-resolved optical coherence tomography and optical Doppler tomography for imaging blood flow in human skin with fast scanning speed and high velocity sensitivity," Opt. Lett. 25, 114-116 (2000).

[85] J. Welzel, "Optical coherence tomography in dermatology: a review," Skin. Res. Technol. 7, 1-9 (2001).

[86] T. Gambichler, A. Pljakic, and L. Schmitz, "Recent advances in clinical application of optical coherence tomography of human skin," Clin. Cosmet. Investig. Dermatol. 8, 345-354 (2015).

[87] N. Greaves, B. Benatar, S. Whiteside, T. Alonso-Rasgado, M. Baguneid, and A. Bayat, "Optical coherence tomography: a reliable alternative to invasive histological assessment of acute wound healing in human skin?" Br. J. Dermatol. 170, 840-850 (2014).

[88] K. Sahu, Y. Verma, M. Sharma, K. Rao, and P. Gupta, "Non-invasive assessment of healing of bacteria infected and uninfected wounds using optical coherence tomography," Skin. Res. Technol. 16, 428-437 (2010).

[89] E. C. E. Sattler, K. Poloczek, R. Kästle, and J. Welzel, "Confocal laser scanning microscopy and optical coherence tomography for the evaluation of the kinetics and quantification of wound healing after fractional laser therapy," J. Am. Acad. Dermatol. 69, e165-e173 (2013).

[90] M. J. Cobb, Y. Chen, R. A. Underwood, M. L. Usui, J. Olerud, and X. Li, "Noninvasive assessment of cutaneous wound healing using ultrahigh-resolution optical coherence tomography," J. Biomed. Opt. 11, 064002 (2006).

[91] J. G. Fujimoto, C. Pitris, S. A. Boppart, and M. E. Brezinski, "Optical coherence tomography: an emerging technology for biomedical imaging and optical biopsy," Neoplasia 2, 9-25 (2000).

[92] G. Zhang, D. J. Moore, C. R. Flach, and R. Mendelsohn, "Vibrational microscopy and imaging of skin: from single cells to intact tissue," Anal. Bioanal. Chem. 387, 1591-1599 (2007).

[93] H. Lui, J. Zhao, D. McLean, and H. Zeng, "Real-time Raman spectroscopy for in vivo skin cancer diagnosis," Cancer. Res. 72, 2491-2500 (2012).

[94] Y. Li, R. Chen, H. Zeng, Z. Huang, S. Feng, and S. Xie, "Raman spectroscopy of Chinese human skin in vivo," Chin. Opt. Lett. 5, 105-107 (2007).

[95] P. Caspers, G. Lucassen, H. Bruining, and G. Puppels, "Automated depth-scanning confocal Raman microspectrometer for rapid in vivo determination of water concentration profiles in human skin," J. Raman Spectro. 31, 813-818 (2000).

[96] H.-W. Wang, T. T. Le, and J.-X. Cheng, "Label-free imaging of arterial cells and extracellular matrix using a multimodal CARS microscope," Opt. Commun. 281, 1813-1822 (2008).

[97] C. L. Evans, E. O. Potma, M. Puoris' haag, D. Côté, C. P. Lin, and X. S. Xie, "Chemical imaging of tissue in vivo with video-rate coherent anti-Stokes Raman scattering microscopy," Proc. Natl. Acad. Sci. U. S. A. 102, 16807-16812 (2005).

[98] M. N. Slipchenko, T. T. Le, H. Chen, and J.-X. Cheng, "High-speed vibrational imaging and spectral analysis of lipid bodies by compound Raman microscopy," J. Phys. Chem. B 113, 7681-7686 (2009).

[99] D. Haluszka, R. Szipocs, N. Wikonkal, and A. Kolonics, "Characterization of obesity in murine skin in vivo by CARS and SHG microscopy using a cost efficient, fiber laser based wavelength extension unit," in 6th EPS-QEOD Europhoton Conference. Neuchatel, Switzerland (2014).

[100] P. D. Pudney, M. Mélot, P. J. Caspers, A. Van Der Pol, and G. J. Puppels, "An in vivo confocal Raman study of the delivery of trans retinol to the skin," Appl. Spectrosc. 61, 804-811 (2007).

[101] M. Weinigel, H. Breunig, M. Kellner-Höfer, R. Bückle, M. Darvin, M. Klemp, J. Lademann, and K. König, "In vivo histology: optical biopsies with chemical contrast using clinical multiphoton/coherent anti-Stokes Raman scattering tomography," Laser Phys. Lett. 11, 055601 (2014).

[102] S. Lange-Asschenfeldt, A. Bob, D. Terhorst, M. Ulrich, J. Fluhr, G. Mendez, H.-J. Roewert-Huber, E. Stockfleth, and B. Lange-Asschenfeldt, "Applicability of confocal

laser scanning microscopy for evaluation and monitoring of cutaneous wound healing," J. Biomed. Opt. 17, 076016 (2012).

[103] M. Rajadhyaksha, M. Grossman, D. Esterowitz, R. H. Webb, and R. R. Anderson, "In vivo confocal scanning laser microscopy of human skin: melanin provides strong contrast," J. Invest. Dermatol. 104, 946-952 (1995).

[104] M. Minsky, "Memoir on inventing the confocal scanning microscope," Scanning 10, 128-138 (1988).

[105] T. Wilson, "The role of the pinhole in confocal imaging system," in *Handbook of Biological Confocal Microscopy*, Springer, New York, pp. 167-182 (1995).

[106] F. Helmchen, and W. Denk, "Deep tissue two-photon microscopy," Nat. Methods 2, 932-940 (2005).

[107] P. Calzavara-Pinton, C. Longo, M. Venturini, R. Sala, and G. Pellacani, "Reflectance confocal microscopy for in vivo skin imaging," Photochem. Photobiol. 84, 1421-1430 (2008).

[108] J. Still, E. Law, K. Klavuhn, T. Island, and J. Holtz, "Diagnosis of burn depth using laser induced indocyanine green fluorescence: a preliminary clinical trial," Burns 27, 364-371 (2001).

[109] M. E. Gschwandtner, E. Ambrózy, S. Marić, A. Willfort, B. Schneider, K. Böhler, U. Gaggl, and H. Ehringer, "Microcirculation is similar in ischemic and venous ulcers," Microvasc. Res. 62, 226-235 (2001).

[110] V. Prabhu, S. B. Rao, E. M. Fernandes, A. C. Rao, K. Prasad, and K. K. Mahato, "Objective assessment of endogenous collagen in vivo during tissue repair by laser induced fluorescence," PloS One 9, e98609 (2014).

[111] V. Prabhu, S. B. Rao, S. Chandra, P. Kumar, L. Rao, V. Guddattu, K. Satyamoorthy, and K. K. Mahato, "Spectroscopic and histological evaluation of wound healing progression following Low Level Laser Therapy (LLLT)," J. Biophotonics 5, 168 (2012).

[112] S.-J. Lin, R.-J. Wu, H.-Y. Tan, W. Lo, W.-C. Lin, T.-H. Young, C.-J. Hsu, J.-S. Chen, S.-H. Jee, and C.-Y. Dong, "Evaluating cutaneous photoaging by use of multiphoton fluorescence and second-harmonic generation microscopy," Opt. Lett. 30, 2275-2277 (2005).

[113] T. Luo, J. Chen, S. Zhuo, K. Lu, X. Jiang, and Q. Liu, "Visualization of collagen regeneration in mouse dorsal skin using second harmonic generation microscopy," Laser Phys. 19, 478-482 (2009).

[114] E. Brown, T. McKee, A. Pluen, B. Seed, Y. Boucher, and R. K. Jain, "Dynamic imaging of collagen and its modulation in tumors in vivo using second-harmonic generation," Nat. Med. 9, 796-800 (2003).

[115] A. Zoumi, A. Yeh, and B. J. Tromberg, "Imaging cells and extracellular matrix in vivo by using second-harmonic generation and two-photon excited fluorescence," Proc. Natl. Acad. Sci. U. S. A. 99, 11014-11019 (2002).

[116] B. R. Masters, P. T. So, and E. Gratton, "Multiphoton excitation microscopy of in vivo human skin: functional and morphological optical biopsy based on three-dimensional imaging, lifetime measurements and fluorescence spectroscopy," Ann. N Y. Acad. Sci. 838, 58-67 (1998).

[117] B. Masters, P. So, and E. Gratton, "Optical biopsy of in vivo human skin: multi-photon excitation microscopy," Lasers Med. Sci. 13, 196-203 (1998).

[118] J. A. Palero, H. S. De Bruijn, H. J. Sterenborg, and H. C. Gerritsen, "Spectrally resolved multiphoton imaging of in vivo and excised mouse skin tissues," Biophys. J. 93, 992-1007 (2007).

[119] L. H. Laiho, S. Pelet, T. M. Hancewicz, P. D. Kaplan, and P. T. So, "Two-photon 3-D mapping of ex vivo human skin endogenous fluorescence species based on fluorescence emission spectra," J. Biomed. Opt. 10, 024016 (2005).

[120] J. Paoli, M. Smedh, A.-M. Wennberg, and M. B. Ericson, "Multiphoton laser scanning microscopy on non-melanoma skin cancer: morphologic features for future noninvasive diagnostics," J. Invest. Dermatol. 128, 1248-1255 (2008).

[121] W. R. Zipfel, R. M. Williams, and W. W. Webb, "Nonlinear magic: multiphoton microscopy in the biosciences," Nat. Biotechnol. 21, 1369-1377 (2003).

[122] A. Gafni, and L. Brand, "Fluorescence decay studies of reduced nicotinamide adenine dinucleotide in solution and bound to liver alcohol dehydrogenase," Biochemistry 15, 3165-3171 (1976).

[123] M. Wakita, G. Nishimura, and M. Tamura, "Some characteristics of the fluorescence lifetime of reduced pyridine nucleotides in isolated mitochondria, isolated hepatocytes, and perfused rat liver in situ," J. Biochem. 118, 1151-1160 (1995).

[124] M. C. Skala, K. M. Riching, A. Gendron-Fitzpatrick, J. Eickhoff, K. W. Eliceiri, J. G. White, and N. Ramanujam, "In vivo multiphoton microscopy of NADH and FAD redox states, fluorescence lifetimes, and cellular morphology in precancerous epithelia," Proc. Natl. Acad. Sci. U. S. A. 104, 19494-19499 (2007).

[125] J. Chen, C. Guo, F. Zhang, Y. Xu, X. Zhu, S. Xiong, and J. Chen, "In-vivo monitoring rat skin wound healing using nonlinear optical microscopy," Proc. of SPIE BiOS (International Society for Optics and Photonics, 2014) San Francisco, California, United States, 894820-894827.

[126] R. Cicchi, S. Sestini, V. De Giorgi, D. Massi, T. Lotti, and F. Pavone, "Nonlinear laser imaging of skin lesions," J. Biophotonics 1, 62-73 (2008).

[127] P. Stoller, K. M. Reiser, P. M. Celliers, and A. M. Rubenchik, "Polarization-modulated second harmonic generation in collagen," Biophys. J. 82, 3330-3342 (2002).

[128] R. Cicchi, D. Kapsokalyvas, V. De Giorgi, V. Maio, A. Van Wiechen, D. Massi, T. Lotti, and F. S. Pavone, "Scoring of collagen organization in healthy and diseased human dermis by multiphoton microscopy," J. Biophotonics 3, 34-43 (2010).

[129] T. Yasui, Y. Tohno, and T. Araki, "Characterization of collagen orientation in human dermis by two-dimensional second-harmonic-generation polarimetry," J. Biomed. Opt. 9, 259-264 (2004).

[130] B. A. Torkian, A. T. Yeh, R. Engel, C.-H. Sun, B. J. Tromberg, and B. J. Wong, "Modeling aberrant wound healing using tissue-engineered skin constructs and multiphoton microscopy," Arch. Dermatol.L 6, 180-187 (2004).

[131] L. Cuttle, M. Nataatmadja, J. F. Fraser, M. Kempf, R. M. Kimble, and M. T. Hayes, "Collagen in the scarless fetal skin wound: detection with Picrosirius-polarization," Wound. Repair. Regen. 13, 198-204 (2005).

[132] G. Deka, K. Okano, W.-W. Wu, and F.-J. Kao, "Multiphoton microscopy for skin wound healing study in terms of cellular metabolism and collagen regeneration," in SPIE BiOS (International Society for Optics and Photonics, 2014), pp. 894820-894820-894827.

[133] P. J. Campagnola, A. C. Millard, M. Terasaki, P. E. Hoppe, C. J. Malone, and W. A. Mohler, "Three-dimensional high-resolution second-harmonic generation imaging of endogenous structural proteins in biological tissues," Biophys. J. 82, 493-508 (2002).

[134] S.-W. Chu, T.-Y. Su, R. Oketani, Y.-T. Huang, H.-Y. Wu, Y. Yonemaru, M. Yamanaka, H. Lee, G.-Y. Zhuo, and M.-Y. Lee, "Measurement of a saturated emission of optical radiation from gold nanoparticles: application to an ultrahigh resolution microscope," Phys. Rev. Lett. 112, 017402 (2014).

IntechOpen